Acta Crystallographica Section D
Biological Crystallography
ISSN 0907-4449

addenda and errata

Crystallographic analysis of human hemoglobin elucidates the structural basis of the potent and dual antisickling activity of pyridyl derivatives of vanillin. Corrigendum

Osheiza Abdulmalik,[a] Mohini S. Ghatge,[b] Faik N. Musayev,[b] Apurvasena Parikh,[c] Qiukan Chen,[a] Jisheng Yang,[a] Ijeoma Nnamani,[d] Richmond Danso-Danquah,[b] Dorothy N. Eseonu,[e] Toshio Asakura,[a] Donald J. Abraham,[b] Jurgen Venitz[c] and Martin K. Safo[b]*

[a]Division of Hematology, The Children's Hospital of Philadelphia, Philadelphia, PA 19104, USA, [b]Department of Medicinal Chemistry, School of Pharmacy, Virginia Commonwealth University, Richmond, VA 23298, USA, [c]Department of Pharmaceutics, School of Pharmacy, Virginia Commonwealth University, Richmond, VA 23298, USA, [d]Department of Psychiatry, Duke University Medical Center, Durham, NC 27710, USA, and [e]Department of Natural and Physical Sciences, School of Mathematics, Science and Technology, Virginia Union University, Richmond, VA 23220, USA

Correspondence e-mail: msafo@vcu.edu

The affiliation of one of the authors of Abdulmalik *et al.* (2011) [*Acta Cryst.* D**67**, 920–928] is corrected.

In the article by Abdulmalik *et al.* (2011) the affiliation of Toshio Asakura is incorrect. The correct affiliation is the Division of Hematology, The Children's Hospital of Philadelphia, Philadelphia, USA, as given above.

References

Abdulmalik, O., Ghatge, M. S., Musayev, F. N., Parikh, A., Chen, Q., Yang, J., Nnamani, I., Danso-Danquah, R., Eseonu, D. N., Asakura, T., Abraham, D. J., Venitz, J. & Safo, M. K. (2011). *Acta Cryst.* D**67**, 920–928.

  doi:10.1107/S0907444911045860

Acta Crystallographica Section D
Biological Crystallography
ISSN 0907-4449

Crystallographic analysis of human hemoglobin elucidates the structural basis of the potent and dual antisickling activity of pyridyl derivatives of vanillin

Osheiza Abdulmalik,[a] Mohini S. Ghatge,[b] Faik N. Musayev,[b] Apurvasena Parikh,[c] Qiukan Chen,[a] Jisheng Yang,[a] Ijeoma Nnamani,[d] Richmond Danso-Danquah,[b] Dorothy N. Eseonu,[e] Toshio Asakura,[d] Donald J. Abraham,[b] Jurgen Venitz[c] and Martin K. Safo[b]*

[a]Division of Hematology, The Children's Hospital of Philadelphia, Philadelphia, PA 19104, USA, [b]Department of Medicinal Chemistry, School of Pharmacy, Virginia Commonwealth University, Richmond, VA 23298, USA, [c]Department of Pharmaceutics, School of Pharmacy, Virginia Commonwealth University, Richmond, VA 23298, USA, [d]Department of Psychiatry, Duke University Medical Center, Durham, NC 27710, USA, and [e]Department of Natural and Physical Sciences, School of Mathematics, Science and Technology, Virginia Union University, Richmond, VA 23220, USA

Correspondence e-mail: msafo@vcu.edu

Received 29 June 2011
Accepted 6 September 2011

PDB References:
Hb–INN-298 complex, 3ic0;
Hb–INN-312 complex, 3r5i.

Vanillin has previously been studied clinically as an antisickling agent to treat sickle-cell disease. *In vitro* investigations with pyridyl derivatives of vanillin, including INN-312 and INN-298, showed as much as a 90-fold increase in antisickling activity compared with vanillin. The compounds preferentially bind to and modify sickle hemoglobin (Hb S) to increase the affinity of Hb for oxygen. INN-312 also led to a considerable increase in the solubility of deoxygenated Hb S under completely deoxygenated conditions. Crystallographic studies of normal human Hb with INN-312 and INN-298 showed that the compounds form Schiff-base adducts with the N-terminus of the α-subunits to constrain the liganded (or relaxed-state) Hb conformation relative to the unliganded (or tense-state) Hb conformation. Interestingly, while INN-298 binds and directs its *meta*-positioned pyridine-methoxy moiety (relative to the aldehyde moiety) further down the central water cavity of the protein, that of INN-312, which is *ortho* to the aldehyde, extends towards the surface of the protein. These studies suggest that these compounds may act to prevent sickling of SS cells by increasing the fraction of the soluble high-affinity Hb S and/or by stereospecific inhibition of deoxygenated Hb S polymerization.

1. Introduction

Functional adult hemoglobin (Hb) comprises two α-globin ($\alpha1\alpha2$) and two β-globin ($\beta1\beta2$) subunits arranged around each other, resulting in a large central water cavity. The α- and β-clefts define the two entry points into the central water cavity. Structural hemoglobinopathies, a consequence of gene variants expressing dysfunctional globin proteins, are among the most common congenital genetic disorders worldwide (Modell & Bulyzhenkov, 1988). Sickle-cell disease (SCD) is the consequence of an A→T substitution at codon 6 of the β-globin gene, resulting in a Glu→Val substitution in the expressed β-globin protein (Modell & Bulyzhenkov, 1988; Bunn & Forget, 1968). Intracellular polymerization of deoxygenated sickle Hb (deoxy-Hb S) into long, rigid and insoluble fibers causes the pathophysiology associated with SCD (Modell & Bulyzhenkov, 1988; Bunn & Forget, 1968), facilitating a cascade of adverse events that include compensatory vasoconstriction, an increase in neutrophil count and the adhesion of red blood cells (RBCs) to tissue endothelium. The clinical condition is characterized by chronic hemolytic anemia, frequent and severe painful crises and multi-system

pathology that impacts nearly every organ. Although various supportive therapies have improved the quality of life of patients with SCD, an efficacious, well tolerated therapeutic option remains elusive. Lack of response in up to 30% of patients, poor tolerance and myelosuppression severely limit the use of hydroxyurea, the only drug that is widely used clinically for SCD therapy (Charache *et al.*, 1995; Platt, 2008).

A vast number of published studies (Nnamani *et al.*, 2008; Abdulmalik *et al.*, 2005; Safo *et al.*, 2004; Abraham *et al.*, 1991; Zaugg *et al.*, 1977; Merrett *et al.*, 1986; Beddell *et al.*, 1984) have focused on the investigation of naturally occurring or synthetic aldehydes as potential therapeutic agents for the treatment of SCD. Two well known examples are 12C79 (or tucaresol; Merrett *et al.*, 1986) and the food flavoring agent vanillin (Abraham *et al.*, 1991) (see Fig. 1). These aldehydes form Schiff-base adducts with the N-terminal Val1α of Hb S to left-shift the oxygen-equilibrium curve (OEC), thereby increasing the the oxygen affinity of Hb. This left-shift of the OEC is advantageous because only the deoxygenated/unliganded form (tense or T state) of Hb S polymerizes, while the oxygenated/liganded form (relaxed or R state) is soluble.

Although relatively nontoxic, the large vanillin dose needed to elicit *in vivo* antisickling therapeutic effects was not clinically acceptable. 12C79 (see Fig. 1), a more potent antisickling agent, required significantly lower therapeutic doses and underwent phase II clinical trials, but was terminated owing to immune-mediated toxicity. Another potent antisickling aldehyde, 5-hydroxymethyl-2-furfural (5-HMF; see Fig. 1), has recently been shown to protect transgenic sickle mice from death from acute pulmonary sequestration of sickle cells under hypoxic conditions (Abdulmalik *et al.*, 2005). Preclinical and phase I clinical antisickling studies of 5-HMF for the treatment of sickle-cell anemia are currently at the planning stages. The atomic interactions between 5-HMF and deoxy-Hb and with liganded Hb (relaxed state in the R2 conformation) have also been reported and showed the compound bound in a symmetry-related fashion at the α-cleft of the central water cavity of the protein (Safo *et al.*, 2004). The liganded R2 quaternary structure is one of several known relaxed-state Hb conformations, including the classical R state that exists in equilibrium (Jenkins *et al.*, 2009; Safo & Abraham, 2005; Safo *et al.*, 2011; Silva *et al.*, 1992; Schumacher *et al.*, 1997).

With the aim of enhancing the antisickling potency of naturally occurring antisickling compounds and lowering the therapeutic dose requirements, we synthesized several pyridyl derivatives of vanillin (INN compounds). We have previously reported the synthesis of these compounds and their effect on the oxygen affinity of normal hemoglobin (Nnamani *et al.*, 2008). In the current study, the functional and antisickling properties of two of the derivatives, INN-312 [5-methoxy-2-(pyridin-3-ylmethoxy)benzaldehyde] and INN-298 [4-methoxy-3-(pyridin-2-ylmethoxy)benzaldehyde] (see Fig. 1) have been further investigated. We have also studied the atomic interactions of INN-312 and INN-298 with both liganded and unliganded Hb to elucidate the structural basis of their potent and/or dual antisickling activities.

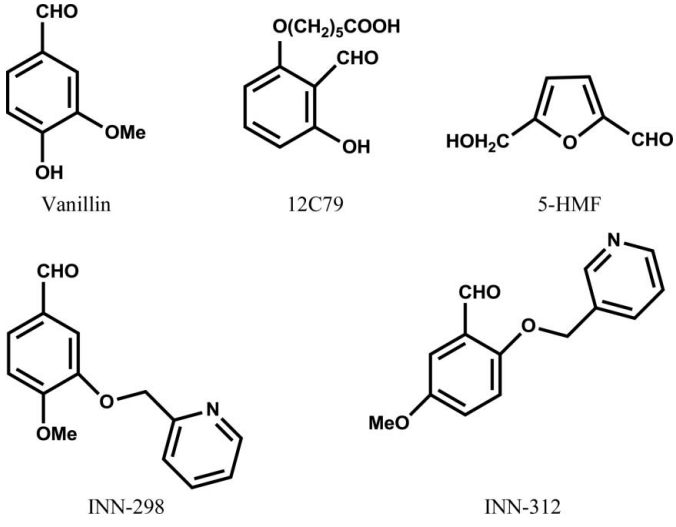

Figure 1
Structures of vanillin, 12C79, 5-HMF and INN compounds.

2. Experimental procedures

2.1. Materials

All chemicals were obtained from Sigma–Aldrich (St Louis, Missouri, USA). INN-312 and INN-298 were synthesized as previously published (Nnamani *et al.*, 2008). De-identified leftover EDTA venous blood samples from patients with SCD who visited The Children's Hospital of Philadelphia for routine clinic visits were obtained after informed consent. Hb was purified from discarded normal blood samples following a published procedure (Safo & Abraham, 2003). The use of these samples is in accordance with the regulations of the IRB for Protection of Human Subjects.

2.2. Oxygen-equilibrium, antisickling and adduct-formation studies

Briefly, suspensions of SS cells in Hemox buffer pH 7.4 containing 10 m*M* glucose and 0.2% bovine serum albumin were pre-incubated under air in the absence or presence of three different concentrations (0.5, 1 and 2 m*M*) of INN-312 and INN-298 at 310 K and then used for oxygen-equilibrium, antisickling and Hb adduct-formation studies as published previously (Abdulmalik *et al.*, 2005) and as also described in detail in the supplementary material[1]. Vanillin was also studied for comparison.

2.3. Sickle Hb solubility studies

The solubility of deoxy-Hb S in 1.7 *M* phosphate buffer pH 7.4, using eight different concentrations of Hb S (0.0025–0.05 g dl^{-1}) and three different INN-312 concentrations (0, 0.5, 1 or 2 m*M*), was measured as previously reported (Fabry *et*

[1] Supplementary material has been deposited in the IUCr electronic archive (Reference: EA5150). Services for accessing this material are described at the back of the journal.

Table 1
Crystallographic data and refinement statistics for the R2-state Hb complex structures.

Values in parentheses are for the outermost resolution bin.

	INN-298	INN-312
Data-collection statistics		
Space group	$P3_221$	$P3_221$
Unit-cell parameters (Å)	$a = b = 92.0$, $c = 143.9$	$a = b = 92.1$, $c = 143.8$
Molecules in asymmetric unit	1 tetramer	1 tetramer
Resolution (Å)	38.75–1.80 (1.86–1.80)	20.51–2.20 (2.28–2.20)
No. of measurements	350101 (37076)	167624 (16583)
Unique reflections	65807 (6480)	36347 (2797)
$\langle I/\sigma(I)\rangle$	14.6 (4.5)	10.5 (3.3)
Completeness (%)	99.9 (100)	99.6 (100)
$R_{\rm merge}$† (%)	5.9 (34.6)	6.7 (34.2)
Structure refinement		
Resolution limits (Å)	27.78–1.80 (1.88–1.80)	20.09–2.20 (2.30–2.20)
σ cutoff (F)	0.0	0.0
No. of reflections	65805 (7700)	36267 (4500)
R factor (%)	20.1 (36.5)	20.9 (26.9)
$R_{\rm free}$‡ (%)	23.0 (38.0)	26.8 (36.0)
R.m.s.d. from standard geometry		
Bond lengths (Å)	0.018	0.011
Bond angles (°)	2.1	1.8
Dihedral angles		
Most favored (%)	92.0	91.4
Allowed regions (%)	7.6	8.4
Average B factors (Å^2)		
All atoms	32.3	46.4
Protein	31.4	45.8
Heme	27.4	43.7
Water	41.8	53.7
INN	37.1	47.4

† $R_{\rm merge} = \sum_{hkl}\sum_i |I_i(hkl) - \langle I(hkl)\rangle| / \sum_{hkl}\sum_i I_i(hkl)$. ‡ $R_{\rm free}$ was calculated with 5% of the reflections, which were excluded from the refinement.

al., 2001, 2003) and as also described in detail in the supplementary material.

2.4. Crystallization and data collection

A freshly prepared solution of INN-312 or INN-298 in 50 m*M* potassium phosphate pH 7.2 buffer was incubated with deoxy-Hb (60 mg ml^{-1} protein) at an Hb tetramer:compound molar ratio of 1:5 and then crystallized with 3.4 *M* sulfate/phosphate pH 6.8 precipitant as previously described for other antisickling aldehydes (Safo *et al.*, 2004). The experiment resulted in two different crystal morphologies for all complexes, which were subsequently determined to be deoxygenated (or T-state) Hb crystals and liganded (or relaxed state in the form of the R2 state) Hb crystals. X-ray diffraction data for the crystals were collected at 100 K using a Molecular Structure Corporation (MSC) X-Stream Cryogenic Cooler System (The Woodlands, Texas, USA), an R-AXIS IV image-plate detector and a Rigaku RU-200 generator (operated at 20 kV and 40 mA). Prior to use in diffraction, the crystals were first washed in a cryoprotectant solution consisting of 30–50 µl mother liquor and 8–12 µl glycerol. The data sets were processed with the MSC *d*TREK* software program and the *CCP*4 suite of programs (Winn *et al.*, 2011). All structure refinements were performed with *CNS* (Brünger *et al.*, 1998). Model building and correction were carried out using the graphics programs *TOM* and *Coot* (Emsley & Cowtan, 2004; Cambillau & Horjales, 1987).

Table 2
Effects of compounds on inhibition of SS cell sickling, oxygen affinity and Hb S adduct formation.

Suspension of SS cells (20% hematocrit). All compounds were solubilized in DMSO (2%). Control experiments without test compound also contained 2% DMSO.

Compound	Concentration (m*M*)	Inhibition of sickling cells (%)	HbS ΔP_{50}† (%)	Hb S adduct formation (%)
INN-312	0.5	15 ± 2	24.8 ± 5.2	34 ± 2.2
INN-312	1	44 ± 10	49.2 ± 5.3	79 ± 2.7
INN-312	2	95 ± 9	75.8 ± 7.9	100 ± 4.9
INN-298	0.5	18 ± 5	7.5	35
INN-298	1	48 ± 7	24.7	55
INN-298	2	80 ± 11	64.5	100
Vanillin	2	0.8 ± 0.2	15 ± 1.9	11.7 ± 3.5
Vanillin	5	12 ± 0.4	40 ± 9.5	40 ± 4.3

† $\Delta P_{50} = [P_{50}(\text{control}) - P_{50}(\text{sample})]/P_{50}(\text{control})$ expressed as a percentage. An OEC study of several INN compounds (at 5 m*M* concentration) with normal blood (40% hematocrit) has previously been reported (Nnamani *et al.*, 2008).

2.5. Structure determination of relaxed-state Hb in complex with INN compounds

Diffraction data from R2-state crystals of the INN-312 and INN-298 complexes were used to calculate difference electron-density maps with *CNS* using phases from the isomorphous R2-state structure (PDB entry 1qxe; Safo *et al.*, 2004) without bound ligands or water. The density map showed INN molecules bound at the α-cleft, as well as the surface of the protein. We also observed bound oxygen molecules at the heme sites. Rigid-body refinement, followed by a series of minimization, annealing, *B*-factor refinement and addition of water molecules, sulfate molecules, heme-bound O_2 and INN molecules with intermittent manual model correction resulted in final R factor and $R_{\rm free}$ values of 20.1% and 23.0%, respectively, for the INN-298 complex (1.8 Å resolution), and 20.9% and 26.8%, respectively, for the INN-312 complex (2.2 Å resolution). The atomic coordinates and structure factors have been deposited in the RCSB Protein Data Bank with accession codes 3ic0 for INN-298 and 3r5i for INN-312. Detailed crystallographic and structural analysis parameters are reported in Table 1. All figures were drawn using *ChemDraw* or *PyMOL* (http://www.pymol.org)

2.6. Structure determination of tense-state Hb in complex with the INN compounds

Diffraction data from T-state crystals of the INN-312 and INN-298 complexes were used to calculate difference electron-density maps using phases from the T-state structure (PDB code 2hhb; Fermi *et al.*, 1984). The respective density maps showed weak and broken density for the bound INN molecules at the α-cleft of the deoxy-Hb. Several cycles of refinement and model fitting with or without a modeled INN compound (at various occupancies) led to even poorer compound electron density. The refinements were then terminated as the structures were indistinguishable from 2hhb. Crystallo-

graphic data and refinement statistics for the partially refined T-state Hb complex structures are reported in Table S1.

3. Results

3.1. INN compounds show highly potent and/or dual antisickling activities

The functional and biological activities of INN-312 and INN-298, together with those of vanillin, were studied by incubating suspensions of SS cells in the absence or presence of 0.5, 1, 2 or 5 m*M* of the test compounds. Table 2 and Fig. S1 show the effects of the various concentrations of the test compounds on the amount of modified Hb S, the degree of left-shift of the OEC and changes in the morphology of SS cells. In all instances, the INN compounds exhibited superior biochemical activities compared with vanillin, with INN-312 being the most potent. The Hb adduct formed is reflected by the amount of modified Hb S in a concentration-dependent manner (Table 2, column 5; Fig. S1*a*). Following the same trend, the compounds left-shifted the OEC in a dose-dependent manner (Table 2, column 4). The degree of shift of the OEC is reported as an increase or decrease in P_{50} (oxygen tension at 50% Hb O_2 saturation). As shown in Fig. S1(*b*), the sigmoidal shape of the curve gradually became hyperbolic with increasing compound concentration, consistent with a reduction in the Hill coefficient of the modified Hb (n = 1.96 for 0.05 m*M*, 1.24 for 1 m*M* and 0.94 for 2 m*M*) compared with that of the control (n = 2.45) and indicating decreased co-operativity among the Hb monomers, which is typical of other Hb modifiers (Abdulmalik *et al.*, 2005; Safo *et al.*, 2004). Congruent to the left-shifting and Hb-modification effects, the compounds significantly reduced the sickling of SS cells, also in a concentration-dependent fashion (Table 2, column 3; Fig. S1*c*).

The solubility of deoxy-Hb S, which is the concentration of fully deoxy-Hb S in equilibrium with polymer (C_{SAT}), is a factor that determines polymer formation *in vivo* (Fabry *et al.*, 2001, 2003). Measurement of C_{SAT} with INN-312 showed a significant elevation in the solubility of deoxy-Hb S, which increased from 0.015 g dl^{-1} (0 m*M* INN-312), to 0.017, 0.025 and >0.05 g dl^{-1} in samples incubated with 0.5, 1 or 2 m*M* INN-312, respectively (Fig. S2).

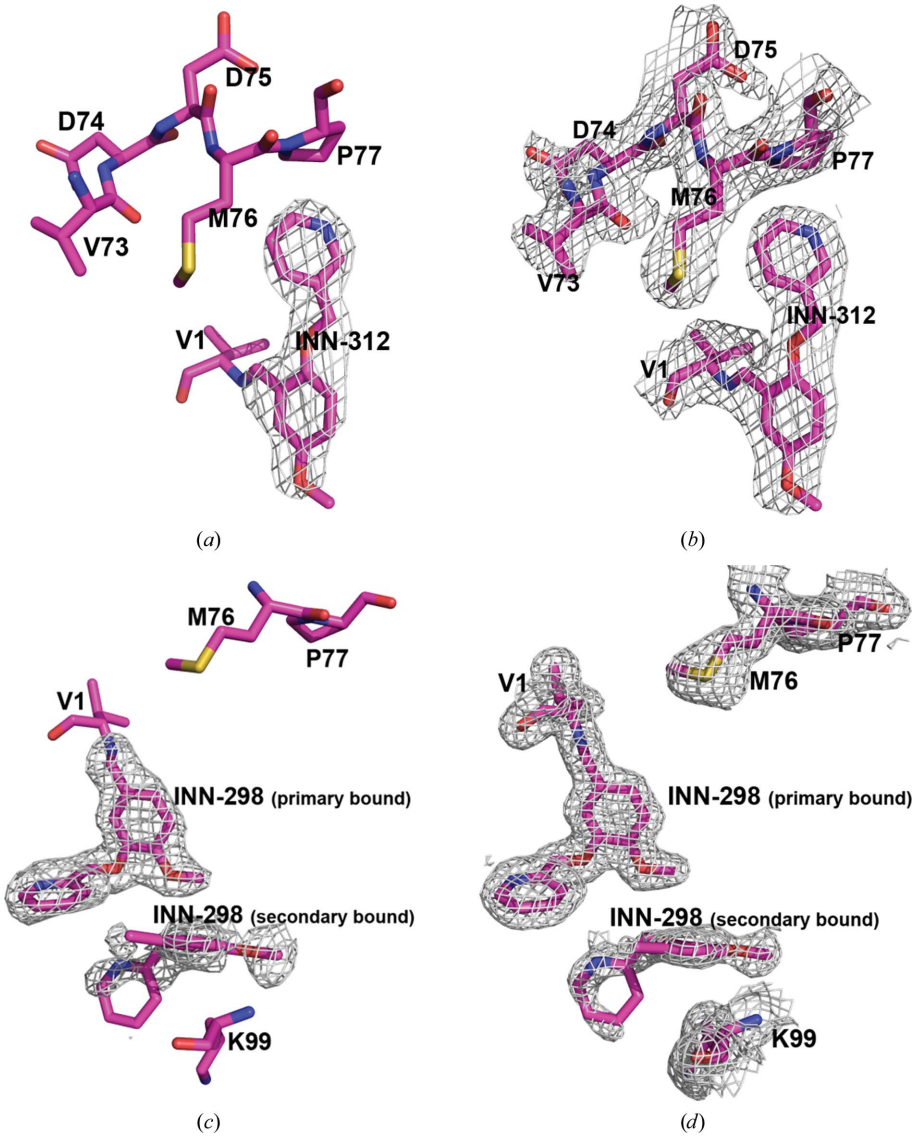

Figure 2
An initial difference electron-density map (with coefficients $F_o - F_c$ shown at the 2.5σ level) of the R2-state INN-312 complex structure before the bound INN-312 molecules at the α-cleft were added to the model. Only one of the two bound molecules is shown. (*b*) A final electron-density map (with coefficients $2F_o - F_c$ shown at the 0.8σ level) of the R2-state INN-312 complex structure. (*c*) An initial difference electron-density map (with coefficients $F_o - F_c$ shown at the 2.2σ level) of the R2-state INN-298 complex structure calculated before the primary and secondary bound INN-298 molecules at the α-cleft were added to the model. (*d*) A final electron-density map (with coefficients $2F_o - F_c$ shown at the 0.8σ level) of the R2-state INN-312 complex structure. All maps are superimposed with the final refined models.

3.2. INN compounds crystallized with both relaxed-state and tense-state Hb

We have determined the crystal structures of INN-298 and INN-312 in complex with unliganded T-state Hb and liganded R2-state Hb to elucidate the structural basis of their antisickling activities. To obtain the cocrystals, Hb (with 1–2% metHb concentration) was deoxygenated under vacuum, incubated with the INN compounds and then crystallized, all under anaerobic conditions. Interestingly, two crystal forms appeared in the same crystallization

setup, which turned out to be unliganded Hb crystals (T-state conformation) belonging to space group $P2_1$ and liganded Hb crystals (relaxed state in the form of the R2-state conformation) belonging to space group $P3_221$. The T-state and R2-state complexes are isomorphous to the native high-salt T-state Hb crystal (PDB entry 2hhb) and native liganded R2-state Hb crystal (PDB entry 1bbb; Silva *et al.*, 1992), respectively, both with a functional tetramer ($\alpha1\beta1\alpha2\beta2$ subunits) in the asymmetric unit.

As noted in §1, the R2 state is part of an ensemble of relaxed-state Hbs that exist in equilibrium in solution (Jenkins *et al.*, 2009; Safo & Abraham, 2005; Safo *et al.*, 2011; Silva *et al.*, 1992; Schumacher *et al.*, 1997). A previous crystallographic study with several other antisickling aldehydes also reported a similar isolation of both T-state and R2-state Hb crystals (Safo *et al.*, 2004). In all the crystallization experiments, the T-state crystals, which are purple in color and rectangular in shape, were the first to appear, in a day or two, and grew to about $0.2 \times 0.3 \times 0.4$ mm in 3–5 d. The second form (R2-state crystals), which were reddish in color and trigonal bipyrimidal in shape, seemed to appear after 1–2 months and normally took about 3–10 months to reach dimensions of $0.1 \times 0.2 \times 0.1$ mm. The predominantly deoxy-Hb solution used for the crystallization experiments may contain partially ligated Hb or even fully ligated Hb in the R2 state. Reaction of the INN compounds with the mixture of T-state Hb and R2-state Hb is believed to destabilize the unliganded Hb but stabilize the liganded Hb, leading to a gradual increase in the R2-state Hb fraction, which eventually crystallizes out, albeit after T-state crystals have appeared several weeks earlier (Safo *et al.*, 2004). Approximately $3–5 \times 10^{-6}$ mol Hb was used for the crystallization setup and it would only take a minute quantity of air in the anaerobic chamber to ligate the Hb. Dissolution of the R2-state crystals showed predominantly oxygenated Hb, with only 5–15% metHb content. The initial difference electron-density maps (before ligand was built at the heme sites) of the R2-state structures also suggested predominantly oxygen molecules bound at all four heme sites. No such heme ligands were observed in the T-state structures. As expected, if a five-molar excess of sodium dithionite (a reducing agent) was added to completely deoxygenate the Hb, as well the exclusion of oxygen from the crystallization medium, only T-state crystals were isolated, demonstrating that oxygen is required to effect the allosteric shift.

3.3. INN compounds bind at the α-cleft of the central water cavity of Hb

The R2-state Hb structures in complex with INN-312 or INN-298 are fully ligated with oxygen, with the structures being indistinguishable (r.m.s.d. of ∼0.4 Å) from the previously published native R2-state liganded structure (PDB entry 1bbb) or the R2-state liganded structure in complex with 5-HMF (PDB entry 1qxe). The heme stereochemistry in the structures is very similar. Similar observations are also found for the corresponding unliganded T-state structures.

In each of the R2-state structures, strong and well defined electron densities (Fig. 2) with full occupancies were identified for a pair of molecules covalently bound to the N-terminal αVal1 residues (Schiff-base interaction) in a symmetry-related fashion. The N-terminal αVal1 binding site is located in the central water cavity of Hb, close to the mouth of the α-cleft. The T-state structures, on the other hand, showed poorly

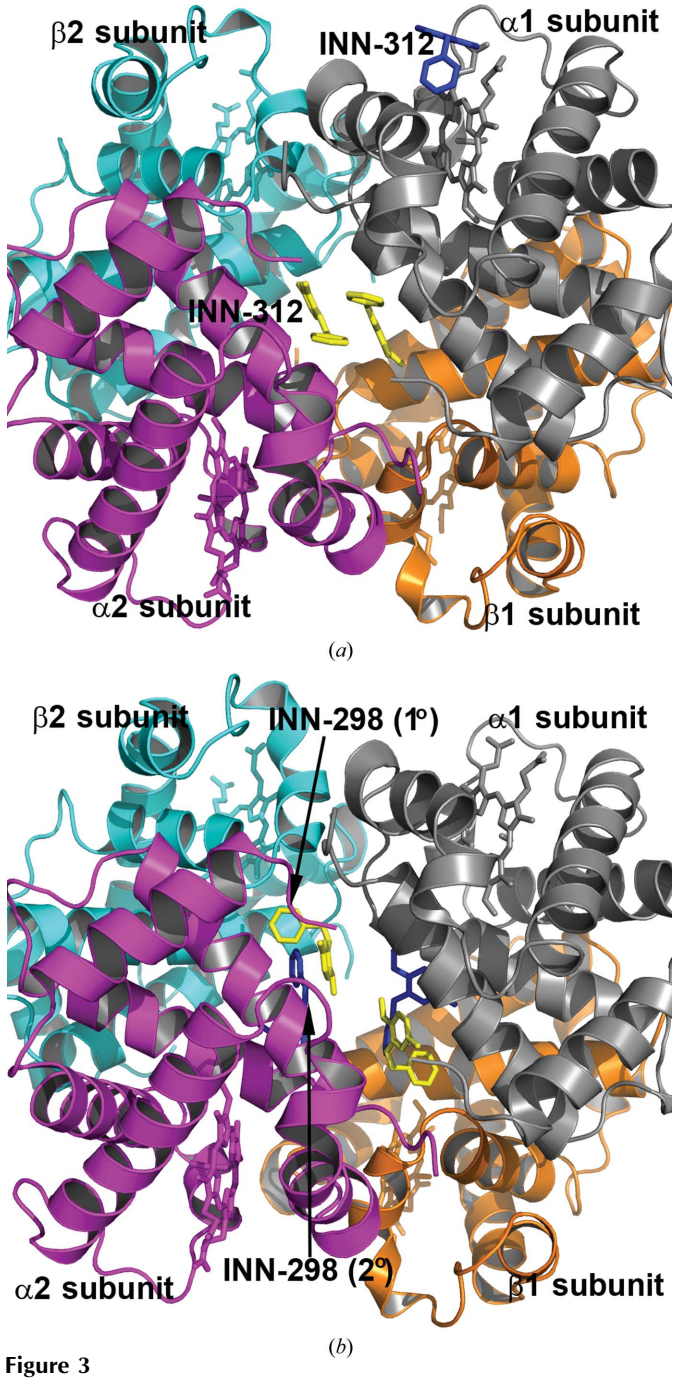

Figure 3
Crystal structures of R2-state Hb in complex with two molecules of INN-312 bound at the α-cleft (yellow sticks) and a third molecule of INN-312 (blue sticks) bound at a surface cavity near the $\alpha1$ heme binding pocket. Hb subunits are shown as ribbons ($\alpha1$ subunit in ash, $\alpha2$ subunit in magenta, $\beta1$ subunit in orange and $\beta2$ subunit in cyan) and hemes are shown as sticks. (*b*) Primary bound (yellow sticks) and secondary bound (blue sticks) INN-298 molecules at the α-cleft in the R2-state structure.

defined compound densities (Fig. S3). Subsequent refinements of the structures with or without the INN compounds made the densities even poorer and as a result the partially refined T-state structures did not include the bound compounds. The weak binding or disorder is likely to be a consequence of the wider α-cleft of the T state preventing a tighter fit of the molecules. The closest distance between the pair of molecules is about 8–9 Å in the T-state structures, compared with about 3–4 Å in the R2-state structures. Previously reported structural studies of other aromatic aldehyde complexes also showed difference compound density in the T-state structures, but were not amenable to refinement (Safo *et al.*, 2004; Abraham *et al.*, 1995; Boyiri *et al.*, 1995). We also identified a second pair of symmetry-related but weakly bound compounds (Figs. 2*c* and 2*d*) in the R2-state INN-298 complex further down the central water cavity. No such density was observed in any of the other structures. There also appears to be a bound INN molecule close to the α1 heme binding pocket in the R2-state structures of both the INN-298 and INN-312 complexes (Fig. 3*a*). This surface binding is most likely to be an artifact since the corresponding α2 heme pocket without any close symmetry Hb molecules lacks this density.

In the R2-state INN-312 complex, the Schiff-base interaction with the α1Val1 N directs the *ortho* pyridine-methoxy substituent (relative to the aldehyde) towards the mouth of the α-cleft, resulting in a direct intrasubunit interaction between the pyridine methoxy O atom and the hydroxyl group of α1Ser131 (Figs. 4*a* and 4*b*). The 3-pyridine N atom makes an intersubunit water-mediated interaction with the amide N atom of α2Leu2. The pyridine ring appears to rotate by 180° with respect to the aryl–C bond, allowing the 3-pyridine N atom to also make alternate intrasubunit water-mediated hydrogen-bond interactions with α1Val73, α1Met76 or α1Asp75. There is also a hydrophobic interaction between the pyridine ring and α1Pro77. The residues αVal73, αAsp75, αMet76 and αPro77 are part of a helix (F-helix) located at the surface of the protein. The 5-methoxy O atom is involved in intersubunit water-mediated hydrogen-bond interactions with the hydroxyl groups of α2Ser138, α2Thr134 or α2Thr137. Note that the other molecule of INN-312 also makes similar, but opposite, interactions with the protein. There are no hydrogen-bond interactions between the pair of INN molecules; however, there is a strong van der Waals contact between the pyridine rings (Fig. 4*b*).

Although the electron density of the bound INN-312 in the T-state structure is poorly defined, it is apparent from the weak density (Fig. S3) that as in the R2-state structure the Schiff-base interaction between INN-312 and αVal1 N in the T-state structure also directs the *ortho*-positioned pyridine-methoxy substituent towards the mouth of the α-cleft, where the pyridine ring makes an obvious hydrophobic contact with αPro77 of the F-helix. The poorly defined INN-312 density in the T-state structure prevents detailed description of the interactions between the compound and the protein. Unlike in the INN-312 complex, the Schiff-base interaction between INN-298 and the protein in both the R2-state and T-state structures directs the *meta*-positioned pyridine-methoxy group further down the central water cavity, although the position of INN-298 in the T-state structure is poorly defined (Fig. S3). The pyridine-methoxy groups of INN-312 and INN-298 are oriented approximately 180° from each other (Fig. 4*c*). As a result, the hydrophobic and/or hydrogen-bond interactions between the pyridine ring and the F-helix observed in the INN-312 complexes are absent. Nevertheless, the pair of INN-298 molecules bound at the α-cleft of the liganded R2-state Hb are involved in several water-mediated interactions involving the 2-pyridine N atom, the 4-methoxy O atom and the 3-pyridine-methoxy O atom with both the α1 and α2 subunits (Lys127, Thr134, Thr137 and Lys139) that tie the two α subunits together (Figs. 4*d* and 4*e*). Like INN-312, the position of INN-298 in the T-state structure is too poorly defined to warrant any detailed analysis of the interactions between this compound and the protein.

The R2-state INN-298 complex structure also showed a pair of weaker secondary INN-298 molecules binding further down the central water cavity (Figs. 3*b* and 4*f*) and making apparent water-mediated and hydrophobic interactions with each other and with the protein (αThr134, αThr137 and αLys99), as well as with the primary bound INN-298 molecules (Fig. 4*f*).

4. Discussion

Benzaldehydes (such as vanillin), as well as furfurals (such as 5-HMF), have been studied as potential therapeutic options for SCD (Abdulmalik *et al.*, 2005; Safo *et al.*, 2004; Abraham *et al.*, 1991; Zhang *et al.*, 2004; Fitzharris *et al.*, 1985). These aldehydes have been shown to form Schiff-base adducts with Hb and to prevent the sickling of SS cells. However, a common disadvantage with these compounds is that high oral doses are likely to be required to elicit acceptable antisickling effects because of the large amount of Hb S (approximately 5 mmol l^{-1}) in the body. Our studies with INN molecules showed significant but varying degrees of left-shifts of the OEC, modification of intracellular Hb S and inhibition of cell sickling, all in a concentration-dependent manner. The INN compounds were significantly more potent than the parent compound vanillin. At a concentration of 1 m*M*, at which most of the compounds inhibited cell sickling by about 40%, vanillin was ineffective. The study also showed that the most potent compound, INN-312, is at least 2.5-fold more potent than 5-HMF *in vitro*. Our C_{SAT} and OEC studies with INN-312 also point to multiple antisickling effects of this compound, *i.e.* it increases the soluble Hb S fraction under partially oxygenated conditions as well as stereospecifically inhibiting direct deoxy-Hb S polymerization under completely deoxygenated conditions.

The structural basis of the antisickling properties of furfurals has been elucidated (Safo *et al.*, 2004). Specifically, it has been observed that the binding of these compounds at the α-cleft of the T state leads to the disruption of salt- and/or water-mediated bridges between the two α-chains, as well as the inhibition of nonspecific chloride ion binding, leading to destabilization of the T-state conformation. In addition, the same compounds were shown to bind to the liganded state, in

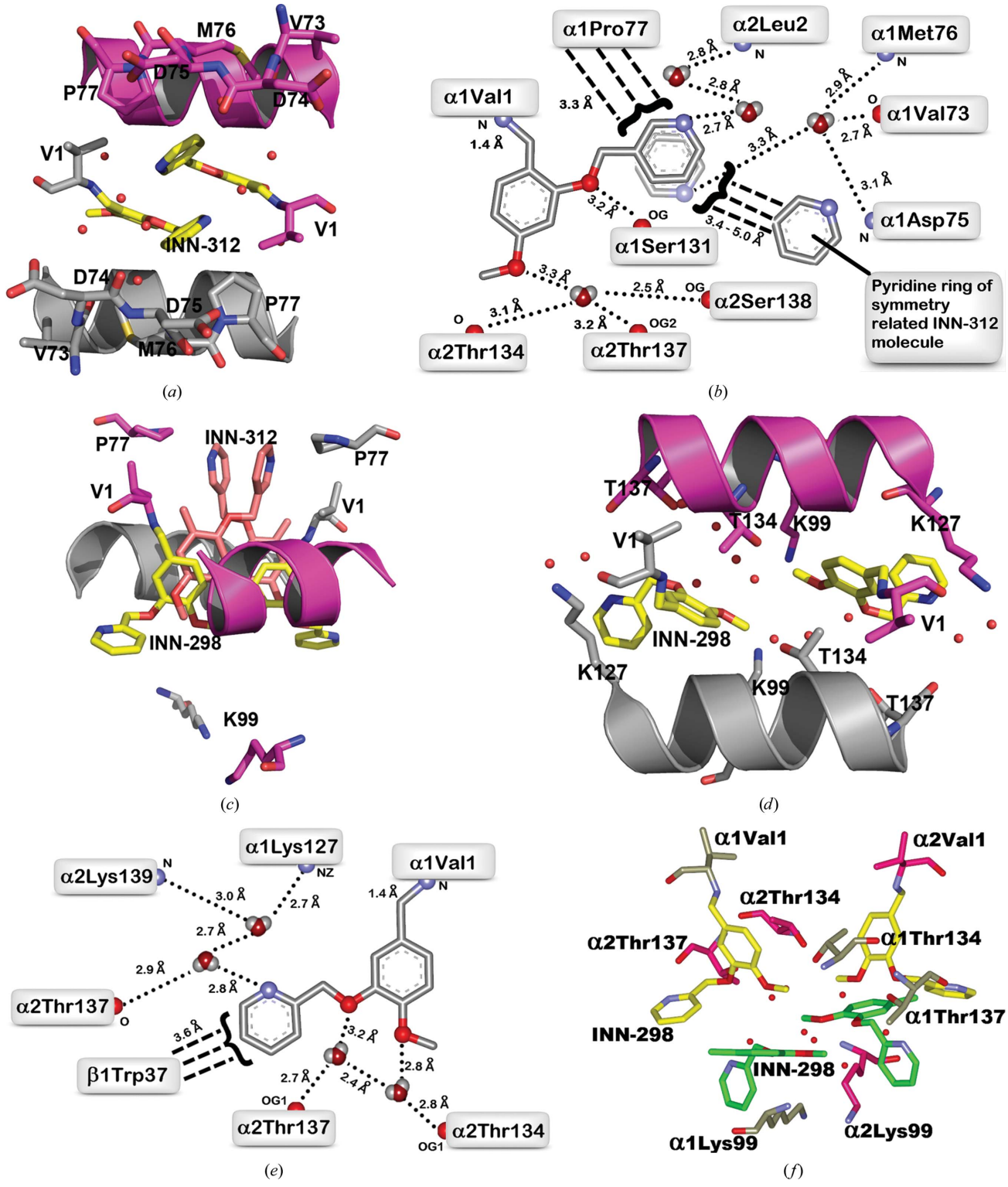

Figure 4
A pair of INN-312 molecules (yellow sticks) bound at the α-cleft of R2-state Hb making Schiff-base interactions with αVal1 N. Hb subunits are shown as sticks or ribbons (α1 subunit in ash, α2 subunit in magenta). Water molecules are shown as red spheres. For brevity, not all residues that make contact with the compound are shown (interacting residues are shown in Fig. 4*b*). (*b*) Two-dimensional contacts between one of the bound INN-312 molecules and the protein at the α-cleft. Small-dashed lines indicate hydrogen-bond interactions and broad-dashed lines indicate hydrophobic contacts. Note the rotation of the pyridine ring with respect to the aryl–C bond, which allows the 3-pyridine N atom to make alternate water-mediated hydrogen-bond contacts with the protein. (*c*) Superimposition of the primary bound INN-298 (yellow) and INN-312 (brown) molecules in R2-state Hb. The protein residues are from the INN-298 structure. (*d*) A pair of INN-298 molecules (yellow sticks) bound at the α-cleft of the R2-state Hb making Schiff-base interactions with αVal1 N. There is a second pair of symmetry-related INN-298 molecules bound further down the central water cavity (see Fig. 4*f*). (*e*) Two-dimensional contacts between one of the primary bound INN-298 molecules and the protein at the α-cleft. (*f*) Primary (yellow sticks) and secondary (green sticks) bound INN-298 molecules.

the form of R2-state Hb, and to stabilize this relaxed conformation through a series of inter-subunit hydrogen-bond and/or hydrophobic interactions. The end result is attenuation of the transition to the T conformation with a concomitant allosteric shift to the relaxed state. This in turn leads to an increased fraction of the more soluble high-affinity Hb. Our studies with INN compounds validate this reported finding. It is obvious that the different molecular interactions of these compounds would be likely to impact on the extent of R2-state stabilization and/or T-state destabilization and could explain the differences in the left-shifting potencies of these compounds.

The solubility studies also suggest that INN-312 could also be acting to directly increase the solubility of deoxy-Hb by stereospecific inhibition of polymer formation. In both the T-state and R2-state structures of the INN-312 complex, the pyridine-methoxy substituent, which is oriented towards the surface of the molecule, makes an apparent water-mediated hydrogen bond and/or hydrophobic contacts with the F-helix (Figs. 4*a*–4*c*). The F-helix residue αAsn78 has been implicated in stabilizing the Hb S fiber and the Hb variant Stanleyville (αAsn78↔αLys78) is known to inhibit gelation (Bunn & Forget, 1968). It is quite possible that the observed contact between INN-312 and the F-helix could lead to destabilization of polymer contact between the Hb S molecules and thus contribute to the antisickling activity of the compounds, which is consistent with the INN-312 $C_{\rm SAT}$ result.

5. Conclusions

The delivery of oxygen to tissues is partly influenced by the affinity of Hb for oxygen. In normal circulation, oxygen is increasingly released in the following order: in larger vessels, at the arterioles and at the capillaries. However, in patients with SCD the existing compensatory low oxygen affinity (P_{50} = 32 ± 2 mmHg; normal P_{50} = 26 ± 2 mmHg) paradoxically causes more oxygen to be released at the arteries and arterioles. Vasoconstriction, which occurs at the arterioles to counteract this process, exacerbates the untoward cell sickling, vasoocclusion and inefficient tissue oxygenation at the capillaries (Winslow, 2004). Aromatic aldehydes are able to increase the oxygen affinity of sickle Hb by stabilizing the relaxed-state Hb conformation relative to the tense-state conformation, ensuring the availability of more oxygen at the capillaries. The release of oxygen at the tissues should not deoxygenate the cells sufficiently for sickling to occur (Winslow, 2004), thus making these compounds viable for use to treat sickle-cell anemia. A second and perhaps more important antisickling mechanism of action is the ability of INN-312 to directly increase the solubility of deoxy-Hb S, which we propose is a consequence of its ability to perturb the surface F-helix, leading to destabilization of polymer formation. Compared with vanillin or 5-HMF, the pyridyl derivatives presented here inhibit *in vitro* sickling and/or gelation at lower concentrations. The potent antisickling effect, coupled with their low molecular weight and their ability to readily pass through the RBC membrane and to interact with intracellular Hb S, as well their direct inhibition of polymer formation, make these compounds attractive drug candidates for further detailed studies as a treatment option for SCD. Our findings also demonstrate the feasibility of a structure–activity approach towards the development of similar compounds with enhanced potency.

We gratefully acknowledge research support from a VCU Presidential Research Initiative Program Award to MKS and JV, an A. D. Williams Research Award to MKS and award No. K01HL103186 from the National Heart, Lung and Blood Institute to OA. The structural biology resources were provided in part by the National Cancer Institute of the NIH to the VCU Massey Cancer Center (grant CA 16059-28). The content is solely the responsibility of the authors and does not necessarily represent the official views of the National Heart, Lung And Blood Institute or the National Institutes of Health.

References

Abdulmalik, O., Safo, M. K., Chen, Q., Yang, J., Brugnara, C., Ohene-Frempong, K., Abraham, D. J. & Asakura, T. (2005). *Br. J. Haematol.* **128**, 552–561.
Abraham, D. J., Mehanna, A. S., Wireko, F. C., Whitney, J., Thomas, R. P. & Orringer, E. P. (1991). *Blood*, **77**, 1334–1341.
Abraham, D. J., Safo, M. K., Boyiri, T., Danso-Danquah, R. E., Kister, J. & Poyart, C. (1995). *Biochemistry*, **34**, 15006–15020.
Beddell, C. R., Goodford, P. J., Kneen, G., White, R. D., Wilkinson, S. & Wootton, R. (1984). *Br. J. Pharmacol.* **82**, 397–407.
Boyiri, T., Safo, M. K., Danso-Danquah, R. E., Kister, J., Poyart, C. & Abraham, D. J. (1995). *Biochemistry*, **34**, 15021–15036.
Brünger, A. T., Adams, P. D., Clore, G. M., DeLano, W. L., Gros, P., Grosse-Kunstleve, R. W., Jiang, J.-S., Kuszewski, J., Nilges, M., Pannu, N. S., Read, R. J., Rice, L. M., Simonson, T. & Warren, G. L. (1998). *Acta Cryst.* D**54**, 905–921.
Bunn, H. F. & Forget, G. B. (1968). *Hemoglobin: Molecular, Genetic and Clinical Aspects*, p. 462. Philadelphia: W. B. Saunders Co.
Cambillau, C. & Horjales, E. (1987). *J. Mol. Graph.* **5**, 174–177.
Charache, S., Terrin, M. L., Moore, R. D., Dover, G. J., McMahon, R. P., Barton, F. B., Waclawiw, M. & Eckert, S. V. (1995). *Control. Clin. Trials*, **16**, 432–446.
Emsley, P. & Cowtan, K. (2004). *Acta Cryst.* D**60**, 2126–2132.
Fabry, M. E., Acharya, S. A., Suzuka, S. M. & Nagel, R. L. (2003). *Methods Mol. Med.* **82**, 271–287.
Fabry, M. E., Desrosiers, L. & Suzuka, S. M. (2001). *Blood*, **98**, 883–884.
Fermi, G., Perutz, M. F., Shaanan, B. & Fourme, R. (1984). *J. Mol. Biol.* **175**, 159-174.
Fitzharris, P., McLean, A. E., Sparks, R. G., Weatherley, B. C., White, R. D. & Wootton, R. (1985). *Br. J. Clin. Pharmacol.* **19**, 471–481.
Jenkins, J. D., Musayev, F. N., Danso-Danquah, R., Abraham, D. J. & Safo, M. K. (2009). *Acta Cryst.* D**65**, 41–48.
Merrett, M., Stammers, D. K., White, R. D., Wootton, R. & Kneen, G. (1986). *Biochem. J.* **239**, 387–392.
Modell, B. & Bulyzhenkov, V. (1988). *World Health Stat. Q.* **41**, 209–218.
Nnamani, I. N., Joshi, G. S., Danso-Danquah, R., Abdulmalik, O., Asakura, T., Abraham, D. J. & Safo, M. K. (2008). *Chem. Biodivers.* **5**, 1762–1769.
Platt, O. S. (2008). *N. Engl. J. Med.* **358**, 1362–1369.
Safo, M. K., Abdulmalik, O., Danso-Danquah, R., Burnett, J. C., Nokuri, S., Joshi, G. S., Musayev, F. N., Asakura, T. & Abraham, D. J. (2004). *J. Med. Chem.* **47**, 4665–4676.
Safo, M. K. & Abraham, D. J. (2003). *Methods Mol. Med.* **82**, 1–19.

Safo, M. K. & Abraham, D. J. (2005). *Biochemistry*, **44**, 8347–8359.
Safo, M. K., Ahmed, M. H., Ghatge, M. S. & Boyiri, T. (2011). *Biochim. Biophys. Acta*, **1814**, 797–809.
Schumacher, M. A., Zheleznova, E. E., Poundstone, K. S., Kluger, R., Jones, R. T. & Brennan, R. G. (1997). *Proc. Natl Acad. Sci. USA*, **94**, 7841–7844.
Silva, M. M., Rogers, P. H. & Arnone, A. (1992). *J. Biol. Chem.* **267**, 17248–17256.
Winn, M. D. *et al.* (2011). *Acta Cryst.* D**67**, 235–242.
Winslow, R. M. (2004). *Transfus. Altern. Transfus. Med.* **5**, 498–504.
Zaugg, R. H., Walder, J. A. & Klotz, I. M. (1977). *J. Biol. Chem.* **252**, 8542–8548.
Zhang, C., Li, X., Lian, L., Chen, Q., Abdulmalik, O., Vassilev, V., Lai, C. S. & Asakura, T. (2004). *Br. J. Haematol.* **125**, 788–795.